



Influence of Formation Temperature on Cycling Stability of Sodium-Ion Cells: A Case Study of Na₃V₂(PO₄)₂F₃|HC Cells

Juan Forero-Saboya, Parth Desai, Roman Healy Corominas, Encarnacion Raymundo-Piñero, Aurélien Canizarès, Dominique Foix, Jean-Marie Tarascon, Sathiya Mariyappan

► To cite this version:

Juan Forero-Saboya, Parth Desai, Roman Healy Corominas, Encarnacion Raymundo-Piñero, Aurélien Canizarès, et al.. Influence of Formation Temperature on Cycling Stability of Sodium-Ion Cells: A Case Study of Na₃V₂(PO₄)₂F₃|HC Cells. *Journal of The Electrochemical Society*, 2023, 170 (10), pp.100529. 10.1149/1945-7111/ad017f . hal-04294713

HAL Id: hal-04294713

<https://univ-pau.hal.science/hal-04294713>

Submitted on 20 Nov 2023

HAL is a multi-disciplinary open access archive for the deposit and dissemination of scientific research documents, whether they are published or not. The documents may come from teaching and research institutions in France or abroad, or from public or private research centers.

L'archive ouverte pluridisciplinaire **HAL**, est destinée au dépôt et à la diffusion de documents scientifiques de niveau recherche, publiés ou non, émanant des établissements d'enseignement et de recherche français ou étrangers, des laboratoires publics ou privés.

Supporting Information

Influence of formation temperature on cycling stability of sodium-ion cells: A case study of $\text{Na}_3\text{V}_2(\text{PO}_4)_2\text{F}_3$ | HC cells.

Juan Forero-Saboya,^{1,2} Parth Desai,^{1,2,3} Roman Healy-Corominas,^{1,2} Encarnacion Raymundo-Piñero,^{2,4} Aurélien Canizarès,⁴ Dominique Foix,^{1,2,5} Jean-Marie Tarascon,^{1,2,3} and Sathiya Mariyappan^{1,2*}

¹ Chimie du Solide et de l'Energie, UMR 8260, Collège de France, Paris 75231 CEDEX 05 France

² Réseau sur le Stockage Electrochimique de l'Energie (RS2E), CNRS FR 3459, Amiens 80039 CEDEX 1, France

³ Sorbonne Université, Paris 75005, France

⁴ Conditions Extrêmes Et Matériaux: Haute Température Et Irradiation CEMHTI, CNRS UPR 3079, Université d'Orléans, Orléans CEDEX 2, France

⁵ IPREM/ECP (UMR5254), Université de Pau, 64053 Pau Cedex 9, France

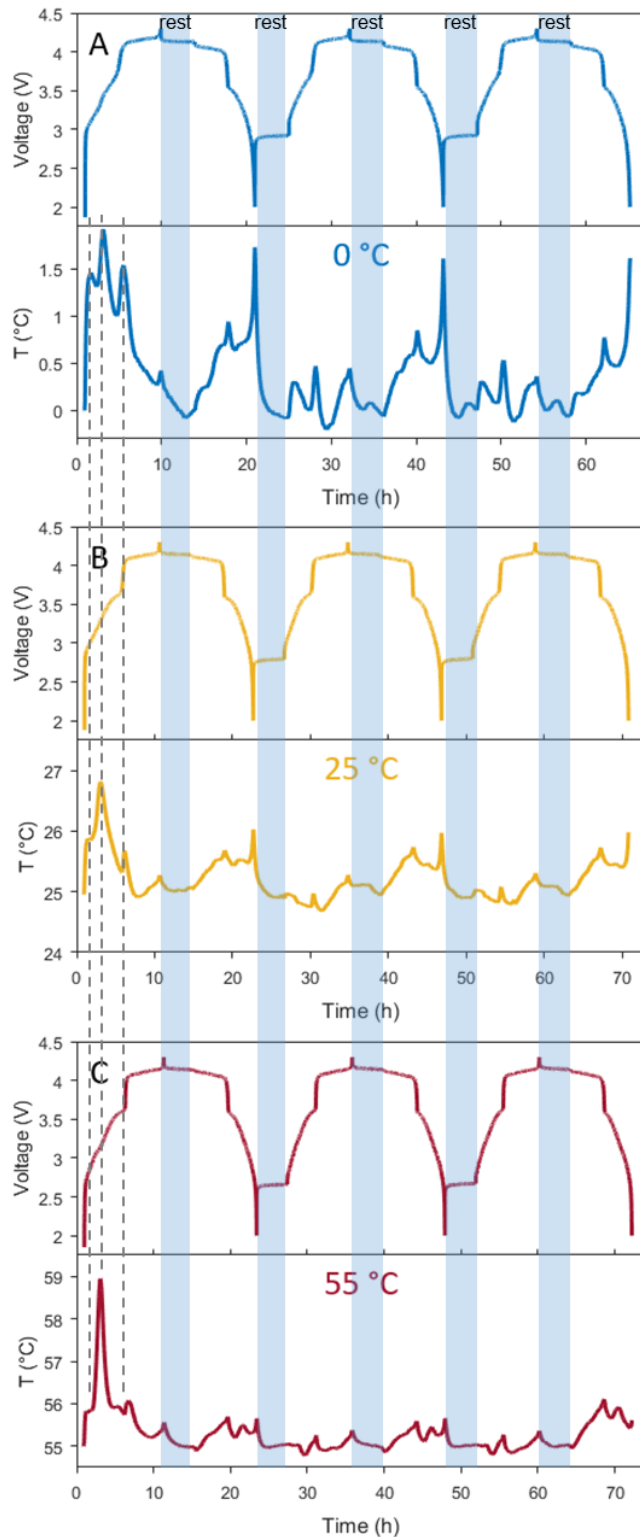


Figure S1. Recorded temperature inside 18650 cells during the three formation cycles, depending on the temperature employed during formation. A) 0 °C, B) 25 °C, and C) 55 °C. The peaks associated to heat release events in the first charge are marked with dashed lines, and the resting regions between charge and discharge are highlighted in light blue.

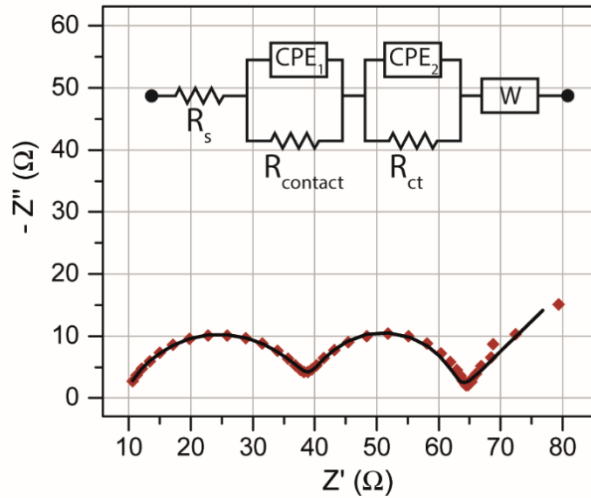


Figure S2. Fitting of the obtained PEIS spectrum right after formation (measured at 100 % SOC and 10 °C). Points represent the obtained experimental data and the black line is the fitted spectrum using the equivalent circuit shown as inset.

Table S1. Parameters obtained for the PEIS fitting procedure, as shown in Figure S2, for the three different formation protocols.

Formation protocol	R_s (Ω)	R_{contact} (Ω)	CPE_1 ($F \cdot s^{a-1}$)	a_1	R_{ct} (Ω)	CPE_2 ($F \cdot s^{a-1}$)	a_2
55x3	9.08	30.49	13.5×10^{-6}	0.748	23.02	0.77×10^{-3}	0.909
25x3	8.43	17.48	4.90×10^{-6}	0.861	15.76	0.97×10^{-3}	0.833
0x3	11.17	14.35	10.5×10^{-6}	0.831	15.45	1.02×10^{-3}	0.884

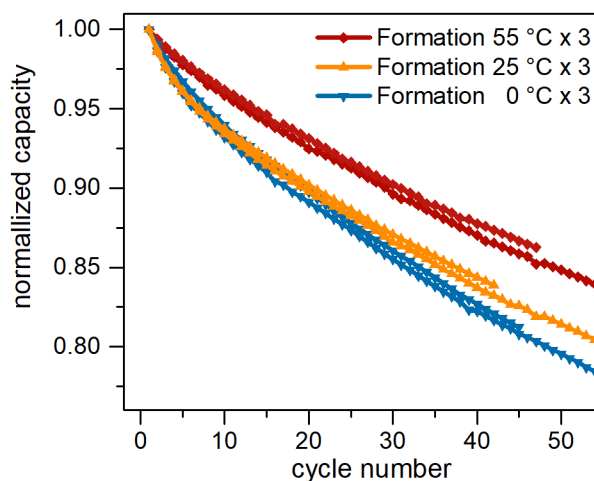


Figure S3. Capacity retention of the NVPF|HC cells depending on the formation protocol used, normalized by the initial discharge capacity of the cell after formation. Two twin cells are presented for each formation.

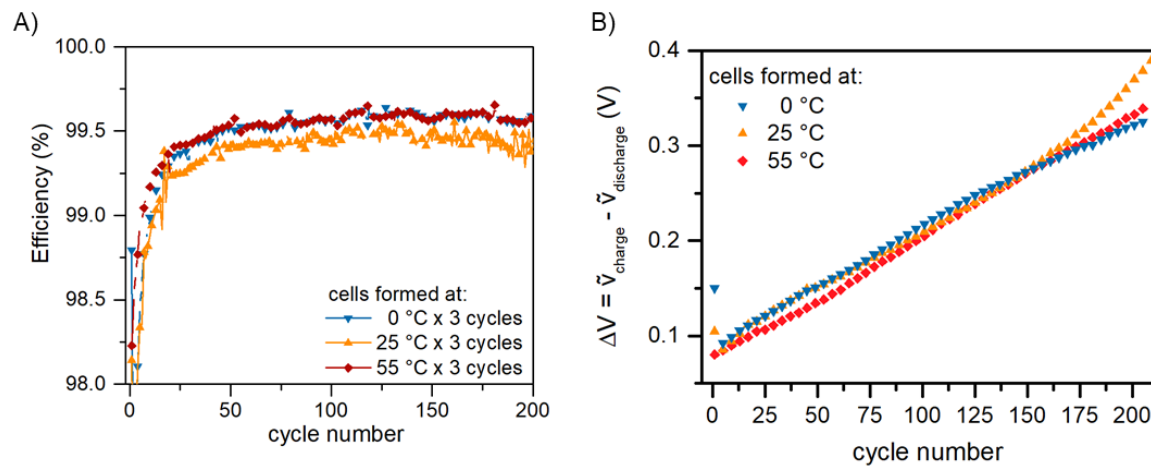


Figure S4. Performance metrics of the NVPF|HC cells as depending on the formation protocol used. A) Coulombic efficiency evolution upon cycling, and B) Evolution of polarization (calculated as the difference between the average voltage during charge and the average voltage during discharge)

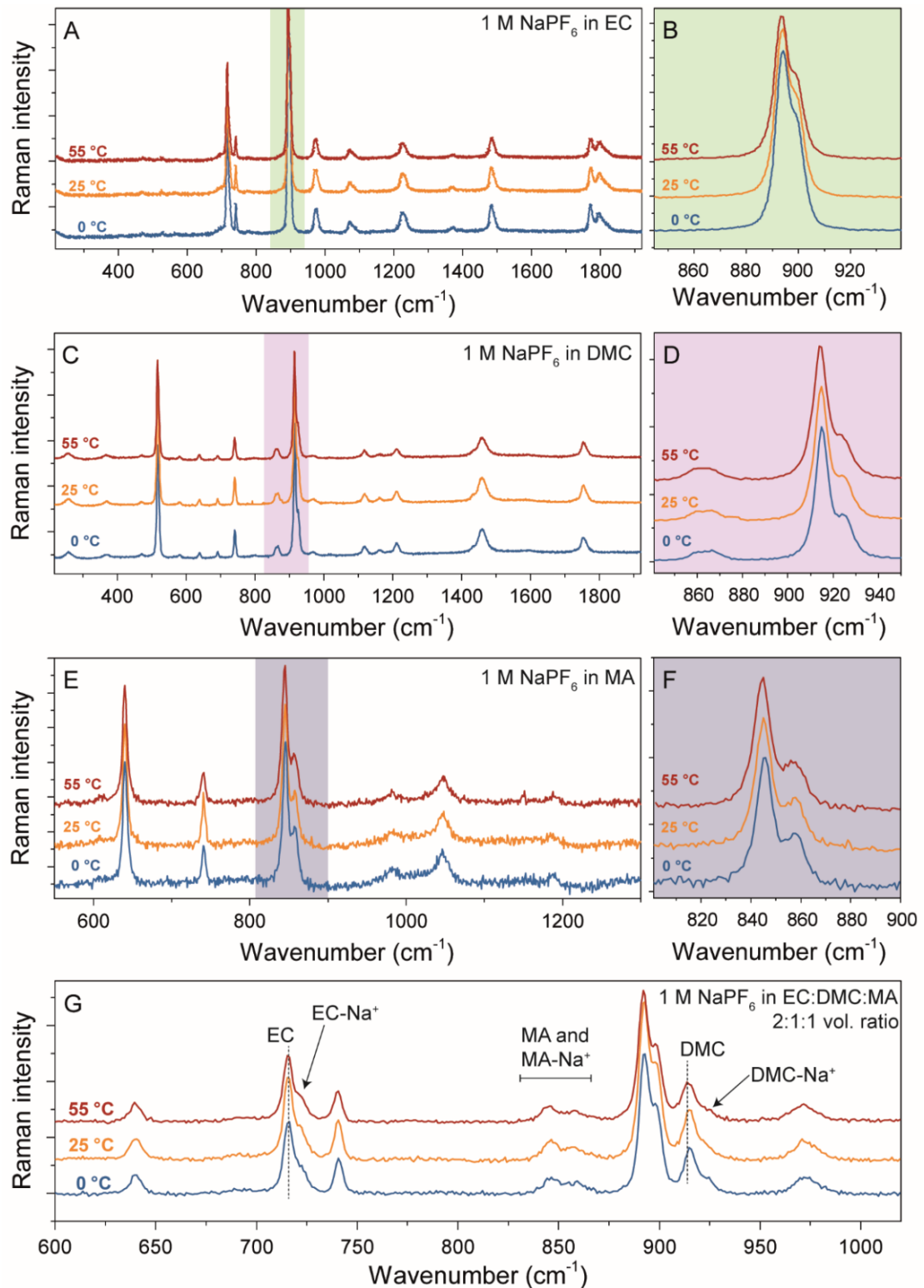


Figure S5. Raman spectra of NaPF_6 electrolytes in different solvent blends, as function of temperature. The solvents in each case EC (panels A and B), DMC (panels C and D), MA (panels E and F), and EC:DMC:MA (panel G). Panels on the right are a zoom in the colored region of the spectra on the left.

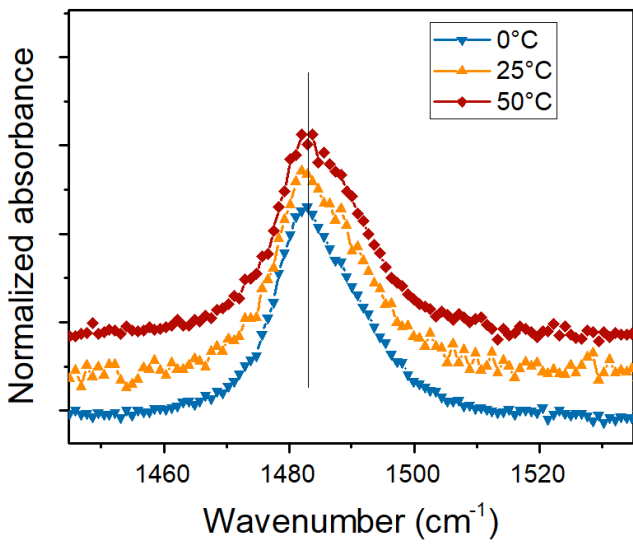


Figure S6. Effect of the temperature on a Raman band of EC. No significant displacement is observed in a solvent upon changes in temperature.

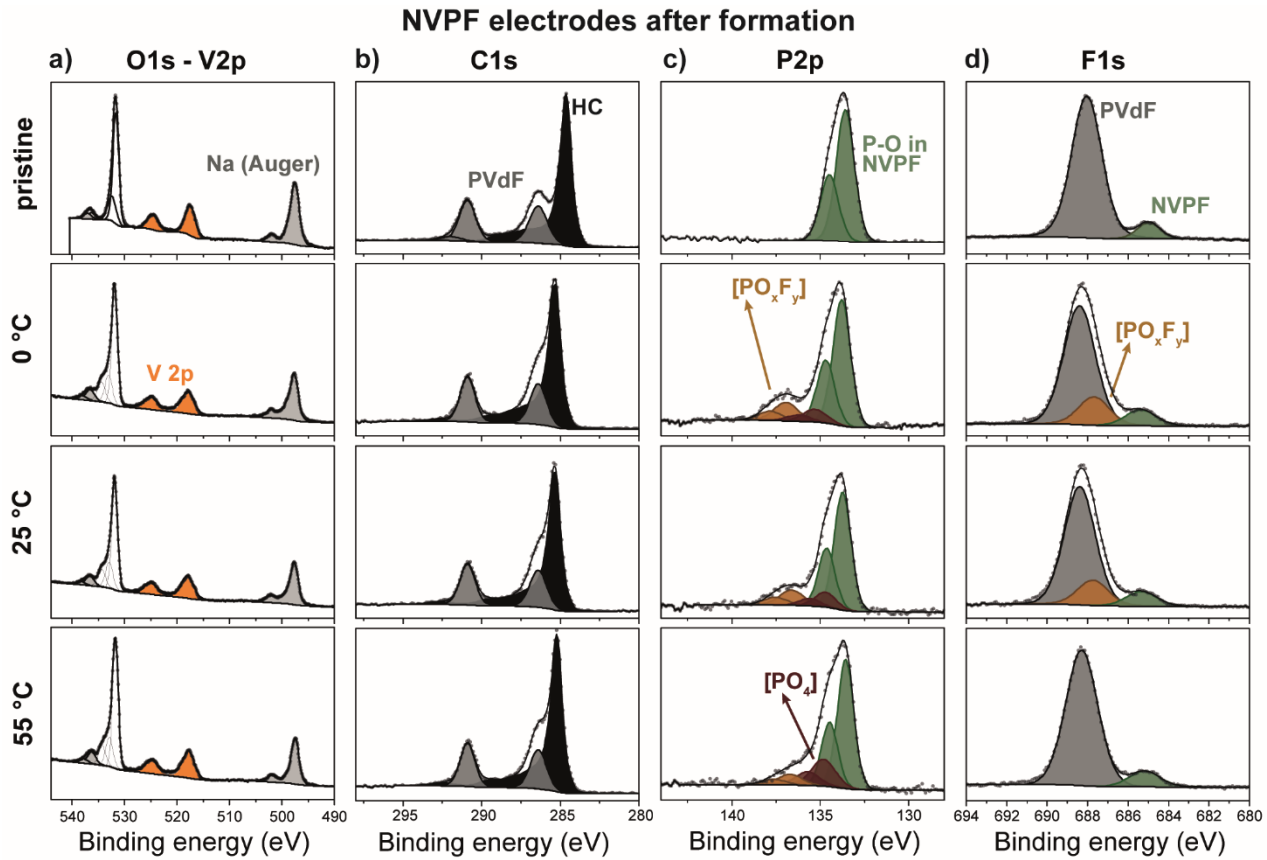


Figure S7. XPS spectra of NVPF electrodes' surface after formation.

Table S2. Integrated intensity of the deconvoluted XPS spectra showed on Figure 5 and Supplementary Figure S6

	C 1s			F 1s		Na 1s	P 2p			V 2p
	HC	PVdF	Deposited C	PVdF + PO _x F _y	NaF	Na	134,0 eV	135,3 eV	137,8 eV	V
HC electrodes	Pristine	51	24	-	20	3,4	-	-	-	-
	0°C	5	6,7	5,1	11,3	25,1	37,6	0,7	0,5	0,8
	25°C	9,3	10	8,4	13,6	20,3	29,6	0,6	0,3	0,6
	55°C Pt1	0,2	0,6	8,2	8,3	25,8	28	4,3	-	0,9
	55°C Pt2	1,1	1,4	5,5	9,5	25	37,9	0,9	1,7	1,2
NVPF electrodes	C black			PVdF + PO _x F _y	NaF	NVPF	133,8 eV	135,3 eV	136,9 eV	V NVPF
	Pristine	38	22	-	23	1,9	2,7	2,9	-	-
	0°C	36,4	19	-	23,2	2,7	2,6	2,7	0,4	0,5
	25°C	37,1	19,1	-	23,1	2,5	2,5	2,7	0,3	0,4
	55°C	38,1	18,6	-	21,5	2,4	2,3	2,8	0,7	-

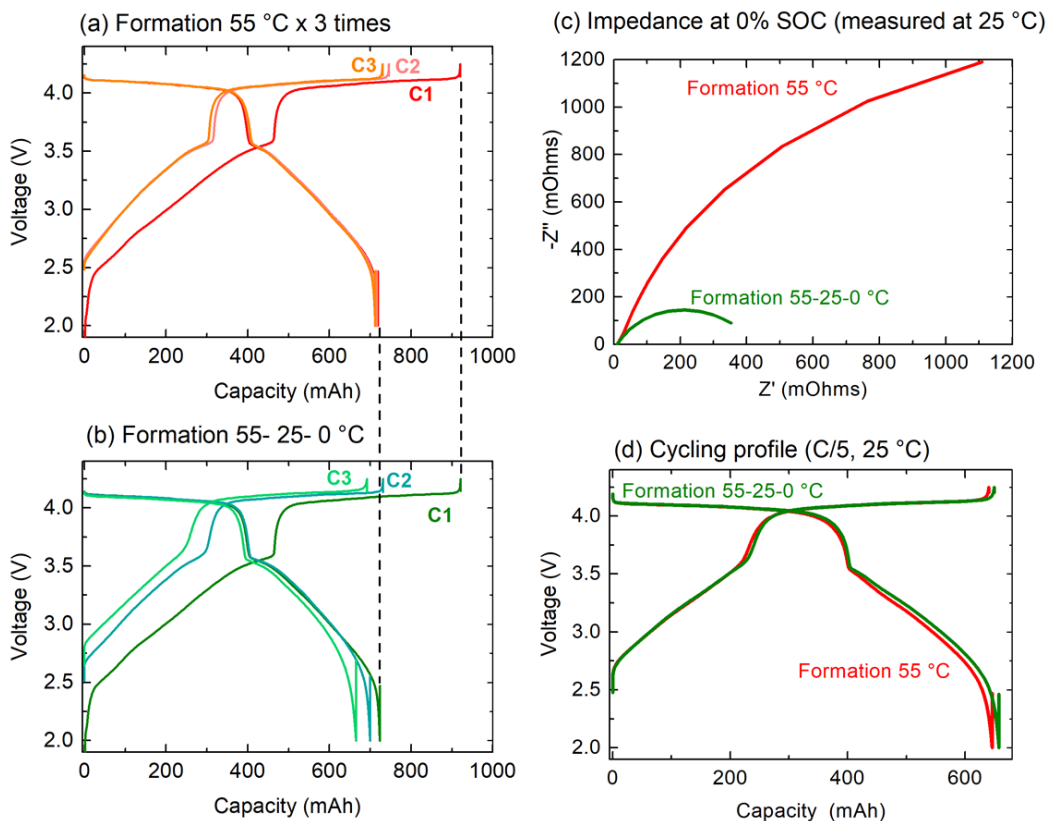


Figure S8. Formation of 18650 NVPF|HC cells. a) Cycling profiles during formation for the 55°C x 3 formation protocol, b) Cycling profiles during the 55-25-0 °C formation protocol, c) Nyquist plot of the cell impedance measured right after formation, at 25 °C and 0 % state of charge (SOC), and d) First cycle of both cells right after formation.

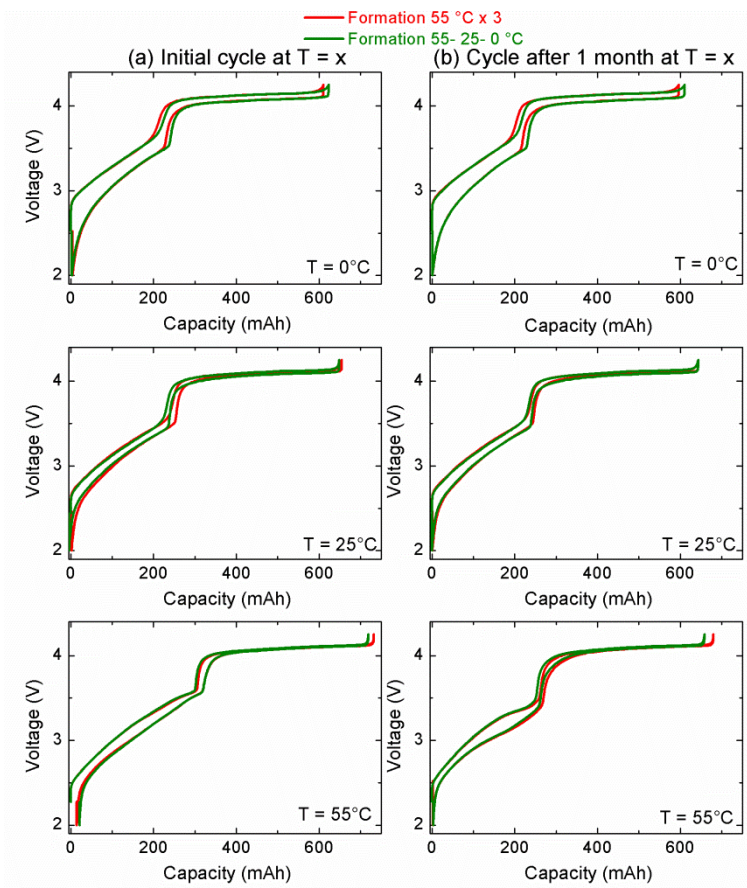


Figure S9. Evolution of the cycling curves of the cells during cycling at different temperatures.

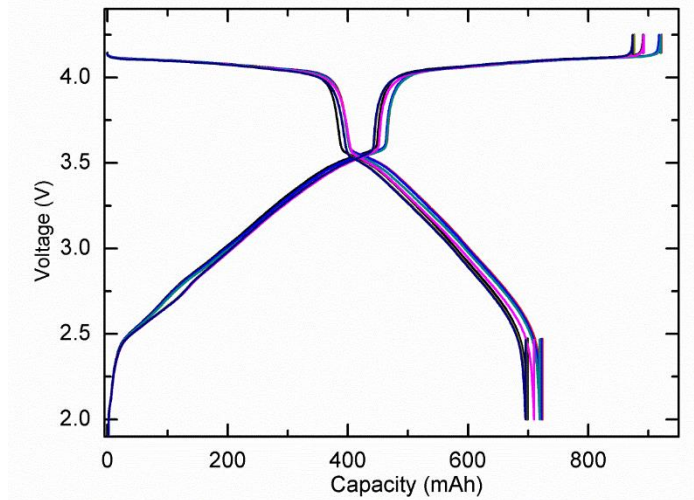


Figure S10. The first cycle profile of the eight 18650 cells used in this study

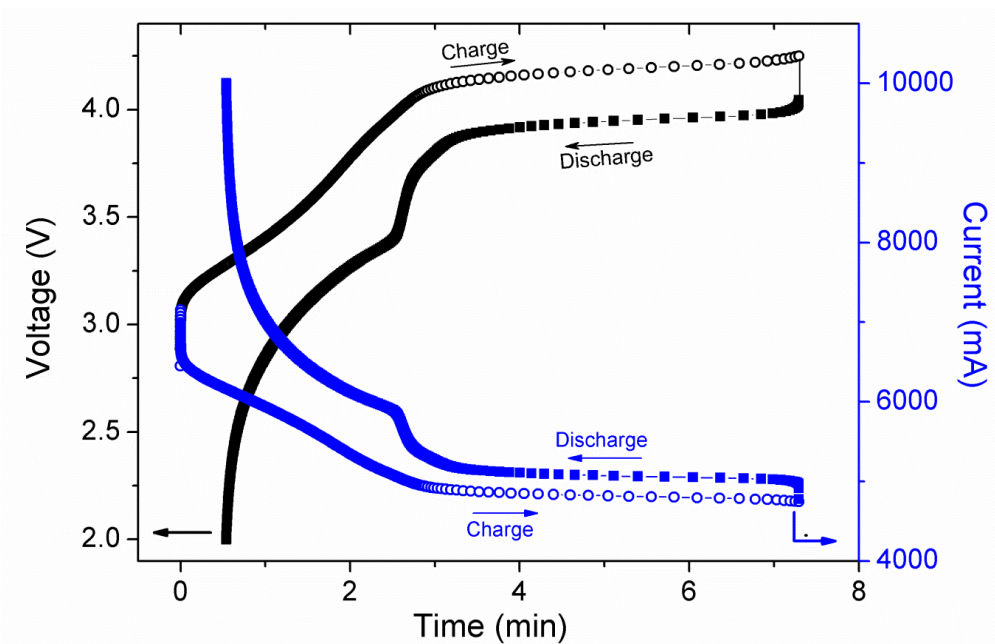


Figure S11. Charge (circles) and discharge (squares) cycling profile of NVPF-HC full cell under constant power protocol with the power of 20 W. The discharge current direction is opposite to that of charge current; however, the absolute number is used here for clarification purposes.